DALTON
FULL PAPER

Biomimetic oxo-, dioxo- and oxo-peroxo-hydrazonato-vanadium(IV/V) complexes†

Mannar R. Maurya,*[a] Shilpa Khurana,[a] Wenjian Zhang[b] and Dieter Rehder[b]

[a] *Department of Chemistry, Indian Institute of Technology, Roorkee 247 667, India. E-mail: rkmanfcy@iitr.ernet.in*
[b] *Institut für Anorganische und Angewandte Chemie, Universität Hamburg, Martin-Luther-King-Platz 6, 20146 Hamburg, Germany. E-mail: dieter.rehder@chemie.uni-hamburg.de*

Received 20th March 2002, Accepted 17th June 2002
First published as an Advance Article on the web 11th July 2002

$[VO(acac)_2]$ reacts with HL (HL is the hydrazone Hacpy-inh **I**, or Hacpy-bhz **II**; acpy = acetylpyridine, inh = isonicotinic acid hydrazide, bhz = benzoylhydrazide) in dry methanol to yield the oxovanadium(IV) complexes [VOL(acac)] (HL = **I**: **1**, HL = **II**: **3**). The dioxovanadium(V) complexes $[VO_2L]$ (HL = **I**: **2**, HL = **II**: **4**) are obtained by aerial oxidation of **1** and **3** in methanol. Treatment of **1** and **3**, or **2** and **4**, with H_2O_2 yields the oxoperoxovanadium(V) complexes $[VO(O_2)L]$ (HL = **I**: **5**, HL = **II**: **6**). In the presence of catechol or benzohydroxamic acid, **1** and **3** give the mixed chelate complexes [VOL(cat)] (HL = **I**: **7**, HL = **II**: **8**) or [VOL(bha)] (HL = **I**: **9**, HL = **II**: **10**). The peroxo complexes **5** and **6** undergo oxygen transfer reaction with PPh_3 in DMF. In DMF and DMSO, **7**, **8**, **9** and **10** slowly convert to the corresponding dioxo species **2** and **4**. Acidification of **2** and **4** with HCl dissolved in methanol affords oxo–hydroxo complexes. Reaction of **7** with L-ascorbic acid yields **2**. The crystal and molecular structures of **2** and **4** have been determined, confirming the *ONN* binding mode of **I** and **II** from their enolate form.

Introduction

Schiff base and related complexes of vanadium, known in a large variety, have received renewed attention in the context of the role of vanadium in living organisms. This resurgence of interest in vanadium chemistry stems from the discovery of two classes of vanadium enzymes, *viz.* vanadium-nitrogenases, containing vanadium in medium oxidation states, and vanadate-dependent haloperoxidases.[1,2] The latter catalyse the oxidation by peroxide of halides to hypohalous acid.[3] Under laboratory conditions, thioethers are oxidized to sulfoxides.[4] The enzymes lose their activity upon reduction or removal of vanadate. Re-oxidation, or reconstitution of the apo-enzyme with vanadate, fully restores their activity,[5] demonstrating that vanadium(V) is essential for the catalytic activity. Intermediate species having $\{VO_2\}$, {VO(OH)}, $\{VO(H_2O)\}$ and $\{VO(O_2)\}$ cores have been proposed during catalytic turnover,[6,7] in which vanadium is in a trigonal-bipyramidal (native form) or tetragonal-pyramidal (peroxo form) environment, covalently linked to the N^{ε} of a histidine. The stability of V^V complexes under aerobic conditions has allowed the design of structural and/or functional models for the haloperoxidases.[2] Vanadium(V) has also been shown to act as an electron acceptor and thus initiator in the photo-cleavage of DNA.[8] Further, many vanadium(V) complexes show haloperoxidase activity[9] and activity in other oxidation and oxo transfer reactions,[6,10] including the enantioselective oxidation of prochiral thioethers to sulfoxides.[11] The insulin like effect of vanadium coordination compounds is another intriguing and promising feature that has further stimulated vanadium coordination chemistry.[12,13]

The objective of the present work is to introduce bio-mimetic dioxovanadium(V) complexes of the hydrazone ligands **I** and **II** (Scheme 1) having pyridine-*N*, enamine-*N* and amide-*O* donor functions, and to study their reactivity with various substrates to characterise species with $\{VO(H_2O)\}$, $\{VO_2\}$, $\{VO(O_2)\}$ and {VO(OH)}cores, similar to those observed for the enzyme. We also report on mixed ligand complexes containing, in addition to **I** and **II**, catecholate or benzohydroxamate. Catacholates and hydroxamates are able to bind vanadium rather strongly in both the +IV and +V oxidation states.[14,15] The relevance of catecholato-vanadium complexes in terms of their biological significance arises from the role of tunichromes in reduction, stabilisation and accumulation of vanadium by certain ascidians (sea squirts);[16] the iron binding siderophore desferrioxamine, which contains hydroxamate functions, also strongly binds to VO^{2+}.[17]

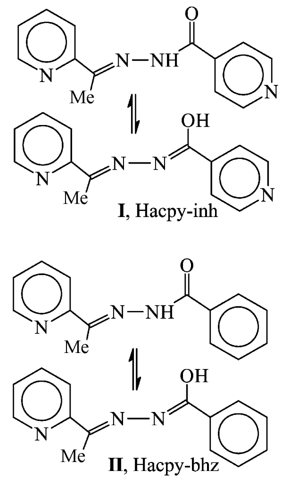

Scheme 1

Experimental

Materials and methods

V_2O_5, $[NH_4][VO_3]$, isonicotinic acid hydrazide (H_2inh), benzoyl chloride, hydrazine hydrate, catechol (H_2cat) and benzo-

† Electronic supplementary information (ESI): table of ^{51}V chemical shifts for **2** and **4**–**10**. See http://www.rsc.org/suppdata/dt/b2/b202852m/

Table 1 Crystal data and structure refinement for $[VO_2(acpy\text{-}inh)]$ (**2**) and $[VO_2(acpy\text{-}bhz)]$ (**4**)

	2	4
Empirical formula	$C_{13}H_{11}N_4O_3V$	$C_{14}H_{12}N_3O_3V$
Formula weight	322.20	321.21
Temperature/K	293(2)	153(2)
Wavelength/Å	0.71073	0.71073
Crystal system, space group	Monoclinic, *C*2/*m*	Monoclinic, *C*2/*c*
a/Å, α/°	14.280(5), 90	16.2827(15), 90
b/Å, β/°	6.834(2), 106.507(6)	12.6396(12), 119.7930(10)
c/Å, γ/°	14.297(5), 90	14.7731(14), 90
Cell volume/Å^3	1337.7(8)	2638.5(4)
Z	4	8
Absorption coefficient/mm^{-1}	0.757	0.766
F(000)	656	1312
Crystal size/mm	0.50 × 0.2 × 0.05	0.40 × 0.15 × 0.10
Reflections collected/unique	3777/1299	15407/3097
R(int)	0.1061	0.0535
Data/restraints/parameters	1299/0/130	3097/0/190
R indices, $[I > 2\sigma(I_0)]$: $R1$, $wR2$	0.0576, 0.1325	0.0468, 0.1234
R indices (all data): $R1$, $wR2$	0.0771, 0.1442	0.0569, 0.1286

hydroxamic acid (H_2bha) were purchased from Loba Chemie, India, acetylacetone (Hacac) and 2-acetylpyridine (acpy) were obtained from Aldrich. $[VO(acac)_2]$ was prepared as described.[18] Benzoylhydrazide (H_2bhz) was prepared by the reaction of a two-fold excess of hydrazine hydrate with ethyl benzoate, which in turn was prepared by refluxing benzoyl chloride in an excess of absolute ethanol. All chemicals and solvents were of analytical grade and used as obtained.

Microanalyses of the ligands and complexes were performed by Regional Sophisticated Instrumentation Center, Central Drug Research Institute, Lucknow, India. Magnetic susceptibilities of the oxovanadium(IV) complexes were recorded at the Institute's Instrumentation Centre IIT, Roorkee. Thermograms of the complexes were recorded on a simple manually operated thermo balance constructed in our laboratory. Crystallised $CuSO_4 \cdot 5H_2O$ was used to calibrate the instrument, and thermograms were recorded under dynamic air atmosphere with a heating rate of 3 to 5 °C min^{-1}. IR spectra were recorded as KBr pellets with a Perkin-Elmer model 1600 FT-IR, and UV–Vis spectra (in DMF) on a UV-1601 PC spectrophotometer. ^1H NMR spectra were run on a Bruker 200 MHz spectrometer, ^{13}C and ^{51}V NMR spectra on a Bruker AM 360 with the common parameters settings. All $\delta(^{51}V)$ values are referenced relative to $VOCl_3$ as external standard. EPR spectra (in DMSO and MeCN) were run in the X-band mode (9.75 MHz) on a Bruker ESP 300E spectrometer.

Crystal structure determinations

Data were collected on a Bruker SMART CCD Apex diffractometer using a graphite monochromator and Mo-K_α radiation (λ = 0.71073 Å) at 153(2) K. Hydrogen atoms were placed in calculated positions and included in the last cycles of refinement. A disorder of C12 and C13 in **2** was accounted for by a 1 : 1 model. Crystal data and details of the data collection and refinement are collated in Table 1. The program systems SHELXS 86 and SHELXL 93 were used throughout.[19]

CCDC reference numbers 182866 and 182867.

See http://www.rsc.org/suppdata/dt/b2/b202852m/ for crystallographic data in CIF or other electronic format.

Preparations

Hacpy-inh I. A mixture of 2-acetylpyridine (1.22 g, 10 mmol) and isonicotinic acid hydrazide (1.37 g, 10 mmol) in 50 ml of methanol was refluxed on a water bath for 6 h. After reducing the solvent to *ca.* 15 ml and cooling to room temp. for 2 h, the precipitated white solid was filtered off, washed with methanol and dried. Recrystallisation from methanol yielded pure **I** as a white solid. Yield 1.92 g (80%). M.p: 160 °C. (Found: C, 64.83, H, 5.10; N, 23.11. Calc. for $C_{13}H_{12}N_4O$: C, 65.0; H, 5.0; N, 23.33). IR (KBr, ν_{max}/cm^{-1}): 3200 (NH), 1661(C=O), 1608, 1573(C=N, C=C).

Hacpy-bhz II. This ligand was prepared by following the same procedure outlined for Hacpy-inh. The pure product was obtained as a white solid. Yield 1.55 g (65 %) on crystallisation from methanol. M.p: 141 °C. (Found: C, 70.35; H, 5.80; N, 17.48. Calc. for $C_{14}H_{13}N_3O$: C, 70.29; H, 5.86; N, 17.57). IR (KBr, ν_{max}/cm^{-1}): 3230 (NH), 1653(C=O), 1622, 1581(C=N, C=C).

[VO(acpy-inh)acac] 1. A stirred solution of Hacpy-inh (0.480 g, 2 mmol) in dry methanol (20 ml) was treated with $[VO(acac)_2]$ (0.530 g, 2 mmol), and the resulting reaction mixture was refluxed on a water bath for 4 h. After cooling to room temp., dark green **1** was filtered off, washed with methanol and dried *in vacuo*. Yield 0.73 g (90%). (Found: C, 53.04; H, 4.48; N, 12.81. Calc. for $C_{18}H_{18}N_4O_4V$: C, 53.33; H, 4.44; N, 13.82). IR (KBr, ν_{max}/cm^{-1}): 1591 (C=N, C=C), 1273 (C–O, enolic), 1022 (N–N), 954 (V=O), 469, 442, 411 (V–O, V–N).

$[VO_2$(acpy-inh)] 2. *Method 1.* **1** (0.405 g, 1 mmol) was dissolved in hot methanol (75 ml) and air was passed through the solution with occasional shaking and heating at *ca.* 50 °C. Residual solid material slowly dissolved, and the green solution gradually changed to yellow; yellow crystalline **2** precipitated within 2 d. This was filtered off, washed with methanol and dried *in vacuo*. Yield 0.229 g (71%). (Found: C, 48.58; H, 3.47; N, 17.19. Calc. for $C_{13}H_{11}O_3N_4V$: C, 48.45; H, 3.42; N, 17.39). IR (KBr, ν_{max}/cm^{-1}): 1598, 1565 (C=N, C=C), 1256 (C–O, enolic), 1022 (N–N), 1025 (N–N), 946, 899 (sym and antisym O=V=O), 507, 441, 421 (V–O, V–N).

Method 2. V_2O_5 (0.500 g, 5 mmol) was suspended in 10 ml of aqueous KOH (containing 0.336 g, 6 mmol) and stirred. The vanadate solution thus generated was filtered after 2 h, and to this was added, under continuous stirring, a filtered solution of Hacpy-inh (1.20 g, 5 mmol) dissolved in 20 ml of aqueous KOH (containing 0.280 g, 5 mmol). The pH of the reaction mixture was slowly adjusted to 7.5 with 4 M HCl, and stirring was continued. After 2 h, the precipitated yellow **2** was filtered off, washed with water and dried. Recrystallisation from DMF–MeOH 1/3 gave 0.810 g (50%) yield of **2**.

[VO(acpy-bhz)acac] 3. Complex **3** was prepared as described for **1** by replacing Hacpy-inh for Hacpy-bhz. Yield 0.69 g (50%). (Found: C, 56.31; H, 4.90; N, 10.25. Calc. for $C_{19}H_{19}N_3O_4V$: C, 56.44; H, 4.70; N, 10.3). IR (KBr, ν_{max}/cm^{-1}): 1596 (C=N, C=C), 1267 (C–O, enolic), 1018 (N–N), 957 (V=O), 494, 442, 415 (V–O, V–N).

[VO_2(acpy-bhz)] 4. This complex was prepared from [VO(acpy-bhz)(acac)] as well as from KVO_3 and Hacpy-bhz by the methods 1 and 2, respectively, as outlined for **2**, in ~55% yield. (Found: C, 52.54; H, 3.96; N, 13.12. Cal. for $C_{14}H_{12}O_3N_3V$: C, 52.34; H, 3.74; N, 13.08). IR (KBr, ν_{max}/cm^{-1}): 1598,1565 (C=N, C=C), 1260 (C–O, enolic), 1028 (N–N), 946, 909 (sym and antisym O=V=O), 509, 472, 441, 410 (V–O, V–N).

[VO(O_2)(acpy-inh)] 5. *Method 1*. A 30% H_2O_2 (2 ml, 17.6 mmol) was added to an aqueous solution of KVO_3 (5 mmol), prepared as outlined in method 2 for **2**, and the resulting solution was stirred at ~10 °C for 1/2 h. Separately, the potassium salt of Hacpy-inh was prepared by reacting **I** (1.2 g, 5 mmol) and KOH (0.280 g, 5 mmol) in 20 ml of water, followed by filtration. This solution was added dropwise to the above solution with constant stirring. After 2 h of stirring, the orange–yellow solid which had separated was filtered off, washed with water and dried. The crude mass was dissolved in a minimum amount of DMF while heating to ~50 °C, and filtered. After treatment with 15 ml of methanol, it was kept at *ca.* 10 °C, whereupon orange crystals of **5** separated. These were filtered off and dried *in vacuo* at ambient temperature. Yield 0.845 g (50%). (Found: C, 45.98; H, 3.19; N, 16.49. Calc. for $C_{13}H_{11}O_4N_4V$: C, 46.15; H, 3.25; N, 16.57). IR (KBr, ν_{max}/cm^{-1}): 1597, 1570 (C=N, C=C), 1260 (C–O, enolic), 1020 (N–N), 956 (V=O), 926 (O–O), 701 (VO_2 antisym), 574 (VO_2 sym), 501, 475, 450, 421 (V–O, V–N).

Method 2. 0.5 mmol of **1** (dissolved in 20 ml of MeOH) or **2** (dissolved in 10 ml of DMF by heating on a water bath) was treated with 30% H_2O_2 (3 ml, 26.5 mmol) while stirred at room temperature, which caused an immediate change of colour to orange–yellow. After 2 h of stirring, the volume was reduced to *ca.* 5ml. In the case of **2** as the precursor, 20 ml of MeOH was added. These solutions were kept at 10 °C overnight. The orange–red crystals were filtered off and dried *in vacuo*. Yield 0.085 g (40%). Analytical and spectral data of the isolated complexes match well with those of compound **5** prepared according to method 1.

[VO(O_2)(acpy-bhz)] 6. This complex was prepared by analogy to **5** (method 1) replacing Hacpy-inh by Hacpy-bhz. Crystallisation from DMF–MeOH as outlined above afforded **6**. Yield 0.925 g (55%). (Found: C, 50.0; H, 4.48; N, 12.37. Calc. for $C_{14}H_{12}O_4N_3V$: C, 49.85; H, 3.56; N, 12.47). IR (KBr, ν_{max}/cm^{-1}): 1598, 1565 (C=N, C=C), 1260 (C–O, enolic), 1022 (N–N), 968 (V=O), 921 (O–O), 714 (VO_2 antisym), 562 (VO_2 sym), 472, 440, 414 (V–O, V–N).

[VO(acpy-inh)cat] 7. 1 mmol of **1** was dissolved in hot methanol (40 ml) and cooled to ambient temp. To this was added catechol (0.110 g, 1 mmol) and the reaction mixture was stirred for 5 h. After reducing the solvent to *ca.* 10 ml and keeping overnight at 10 °C, dark brown complex **7** was filtered off and dried *in vacuo*. Yield 0.21 g (50%). (Found: C, 55.22; H, 3.49; N, 13.41. Calc. for $C_{19}H_{15}N_4O_4V$: C, 55.08; H, 3.62; N, 13.53). IR (KBr, ν_{max}/cm^{-1}): 1591, 1572 (C=N, C=C), 1274 (C–O, enolic), 1029 (N–N), 951 (V=O), 467, 440, 412 (V–O, V–N).

[VO(acpy-bhz)cat] 8. Complex **8** was prepared analogously to **7**, replacing **1** by **3**. Yield 0.226 g (55%). (Found: C, 58.24; H, 3.76; N, 9.93. Calc. for $C_{20}H_{16}N_3O_4V$: C, 58.11; H, 3.87; N, 10.17). IR (KBr, ν_{max}/cm^{-1}): 1598, 1578 (C=N, C=C), 1272 (C–O, enolic), 1022 (N–N), 951 (V=O), 468, 452, 417 (V–O, V–N).

[VO(acpy-inh)bha] 9. 1 mmol of **1** was dissolved in 40 ml of hot methanol and to this, after cooling to ambient temp., was added benzohydroxamic acid (0.137 g, 1 mmol). The obtained reaction mixture was stirred for 4 h and then kept overnight at 10 °C after reducing the volume to *ca.* 10 ml. Complex **9** was filtered off, washed with methanol and dried *in vacuo*. Yield 0.24 g (55%). (Found: C, 54.21; H, 3.96; N, 15.68. Calc. for $C_{20}H_{17}N_5O_4V$: C, 54.30; H, 3.85; N, 15.84). IR (KBr, ν_{max}/cm^{-1}): 1597, 1573 (C=N, C=C), 1235 (C–O, enolic), 1029 (N–N), 965 (V=O), 552, 462, 432 (V–O, V–N).

[VO(acpy-bhz)bha] 10. This was prepared following the procedure outlined for **9**. Yield 0.21 g (48%). (Found: C, 57.35; H, 4.16; N, 12.57. Calc. for $C_{21}H_{18}N_4O_4V$: C, 57.14; H, 4.08; N, 12.70). IR (KBr, ν_{max}/cm^{-1}): 1600, 1564 (C=N, C=C), 1261 (C–O, enolic), 1026 (N–N), 959 (V=O), 509, 452, 422 (V–O, V–N).

Reaction of 5 and 6 with PPh_3

PPh_3 (0.195 g, 0.75 mmol) was added to complex **5** or **6** (0.170 g, 0.5 mmol) dissolved in 15 ml of hot DMF, and the reaction mixture was digested on a water bath for 8 h. After reducing the volume of the solvent to *ca.* 5 ml, methanol (15 ml) was added, and the solution kept at 10 °C, whereupon crystalline solid separated out within 4–6 h. This was filtered off and dried *in vacuo*. Yield: 50%. Analytical and spectral data of the complexes thus obtained matched well with **2** and **4**, respectively.

Results and discussion

Scheme 2 provides an overview of the complexes described in this contribution. Structural formulae are based on structural evidence (*vide infra*) and plausibility.

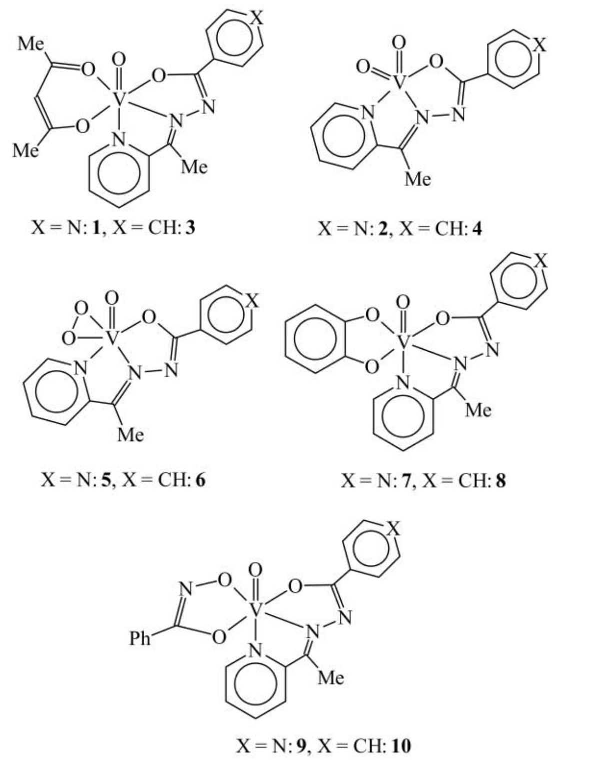

Scheme 2

Synthesis and solid state characteristics

Synthesis. Reaction between equimolar amounts of [VO(acac)$_2$] and Hacpy-inh (**I** in Scheme 1) in dry, refluxing methanol yields [VO(acpy-inh)acac], **1**. Here, as in all of the complexes formed with **I** and **II**, the ligand reacts out of its enolic tautomeric form, *i.e.* in the *NNO*(1−) mode. On aerial oxidation in methanol, the dioxovanadium(v) complex

$[VO_2(acpy\text{-}inh)]$, **2**, is obtained, a reaction which requires water. The intermediate green complex **1** can be isolated from the methanolic solution prior to aeration. Eqns. (1) and (2) represent the synthetic procedures:

$$[V^{IV}O(acac)_2] + Hacpy\text{-}inh \longrightarrow [V^{IV}O(acpy\text{-}inh)acac] + Hacac \quad (1)$$

$$2[V^{IV}O(acpy\text{-}inh)acac] + 1/2\ O_2 + H_2O \longrightarrow 2[V^{V}O_2(acpy\text{-}inh)] + 2Hacac \quad (2)$$

Similarly, the complex [VO(acpy-bhz)acac], **3**, can be oxidised in methanol to $[VO_2(acpy\text{-}bhz)]$, **4**. Further, **2** and **4** were obtained from the reaction of vanadate, prepared *in situ* by dissolving V_2O_5 in an aqueous solution of KOH, by addition of solutions of the potassium salt of **I** or **II**, and after adjustment to pH ~ 7.5. Aqeuous vanadate solutions actually contain a mixture of mono-, di-, tetra- and pentavanadates.[20,21] Addition of H_2O_2 to **1** and **3** yields the peroxo complexes **5** and **6**, eqn. (3). The complexes $[VO(O_2)L]$ (HL = **I** or **II**, **5** or **6**) can also be prepared from aqueous solutions of potassium metavanadate, hydrogen peroxide and the potassium salts of the ligands, as symbolically depicted in eqn. (4). The actual vanadium precursor probably is *in situ* generated $[VO(O_2)_2(OH/H_2O)_x]^{n-}$.[21]

$$2[VO(acac)L] + 3\ H_2O_2 \longrightarrow 2\ [VO(O_2)L] + 2\ Hacac + 2\ H_2O \quad (3)$$

$$KL + KVO_3 + H_2O_2 \longrightarrow [VO(O_2)L] + 2\ KOH \quad (4)$$

(HL = **I**: **5**; HL = **II**: **6**)

Oxo-monoperoxo complexes may further be generated by treating *cis*-dioxo-vanadium(v) complexes with H_2O_2 at ice temperature. This reaction was studied by electronic absorption spectrophotometry. The spectral changes obtained during the reaction (Fig. 1) include a shift of the 370 nm band of **1** to 385 nm in **5**, and the appearance of a weak shoulder at ~410 nm. The rate at which peroxo complex formation occurs depends upon the amount of H_2O_2 added. The band at 243 nm becomes relatively sharp while the band at 282 nm slowly shifts to 273.5 nm. The feature of the final spectrum is similar to that of authentic **5** (see below).

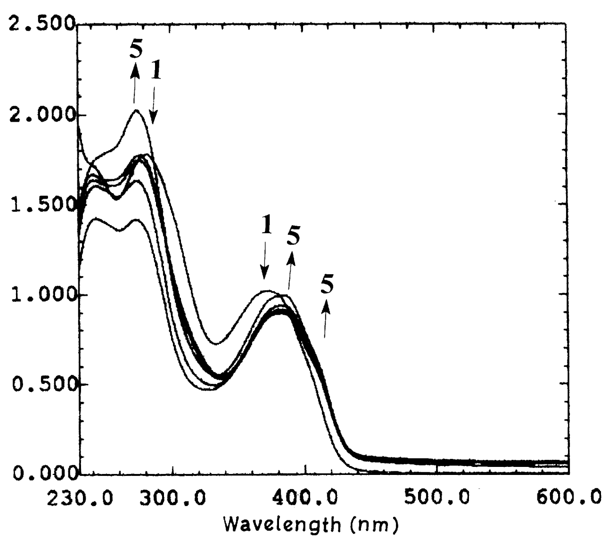

Fig. 1 Titration of [VO(acpy-inh)acac] (**1**) with 30% H_2O_2; the spectra were recorded after the successive addition of two-drop portions of H_2O_2 to 5 ml of *ca.* 10^{-4} M solution of **1** in MeOH.

The peroxo complexes undergo oxygen transfer reactions with PPh_3 in DMF to give the corresponding dioxovanadium(v) complexes $[VO_2L]$, **2** and **4**; Scheme 3.

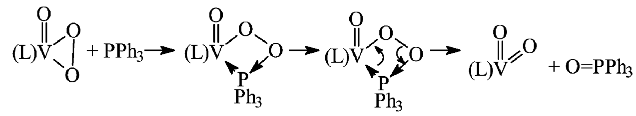

Scheme 3

Treatment of **1** and **3** with catechol or benzohydroxamic acid in methanol under aerobic conditions leads to the formation of the mixed-ligand complexes **7**, **8**, **9** and **10** as represented by eqns. (5) and (6). During this reaction, oxidative replacement of the remaining acetylacetonato group by catecholate or benzdydroxamate takes place.

$$2[V^{IV}OL(acac)] + 2H_2cat + 1/2O_2 + 2H^+ \longrightarrow 2[V^{V}OL(cat)] + 2Hacac + H_2O \quad (5)$$

$$2[V^{IV}OL(acac)] + 2H_2bha + 1/2O_2 + 2H^+ \longrightarrow 2[V^{V}OL(bha)] + 2Hacac + H_2O \quad (6)$$

Complexes **1** and **3** are paramagnetic with a magnetic moment of 1.89 and 1.96 BM, respectively, while the other complexes are diamagnetic as expected for 3d° systems. The dioxo complexes **2** and **4**, and the peroxo complexes **5** and **6** are soluble in DMF and DMSO only, while the other complexes also dissolve in methanol and ethanol. Complexes **7** to **10** are also soluble in CH_2Cl_2.

Thermal studies. The TGA profiles of the VO^{2+} complexes **1** and **3** show that these complexes lose acetylacetone, one oxygen remaining attached to vanadium, between 200 and 275 °C, with concomitant formation of $[V^{V}O_2L]$ as shown by eqn. (7).

$$[V^{IV}O(acac)L] \longrightarrow [V^{V}O_2L] + \{acac - O\} \quad (7)$$

On further heating, $[VO_2L]$ decomposes in the presence of air to yield V_2O_5. The peroxo complexes **5** and **6** degrade in the temperature range 120–220 °C, the decrease of weight by ~9.5% corresponding to the loss of the peroxo group (calcd. 9.5%). Thermograms of the other complexes indicate continuous degradation to V_2O_5 in the 250–700 °C temperature range.

Structure description. The crystal structure of $[VO_2(acpy\text{-}inh)]$ (**2**) and $[VO_2(acpy\text{-}bhz)]$ (**4**) with atom numbering schemes are shown in Fig. 2, selected bond lengths and angles in Table 2. In **2**, a mirror plane bisecting the angle O1–V1–O1# contains all of the other atoms except of the pyrinine carbons C13 and C12, which are disordered so as to satisfy the symmetry conditions (O1# in **2** corresponds to O3 in **4**). The N_2O_3 coordination sphere around the vanadium atom is defined by the pyridine-N, imine-N and the amide-O of the monobasic tridentate ligand acpy-inh/bhz(1−), and by two *cisoid* oxo-groups. The three ligand functions occupy *meridional* positions. The bond distances N2–N3 [1.384(5), 1.381(3)], N3–C8 [1.311(6), 1.314(3)] and O3–C8 [1.296(6), 1.300(3) Å] are consistent with the enolate form of the amide functionality. The V=O distances of 1.615 and 1.618 Å are typical of non-hydrogen bonded V=O groups.[22] Other bond lengths, *e.g.* *d*(V–N1), *d*(V–N2) and *d*(V–O3), are in accord with reported values for comparable complexes.[23,24] The ligand forms two five-membered rings with bite angles of 72.96° (N1–V–N2) and 73.56° (O2–V–N2). With an N1–V–O2 angle of 146.51°, N1 and O2 are inclined towards N2.

The coordination geometry around vanadium can best be described as distorted square-pyramidal with one of the doubly bonded oxo groups (O3), the enolate oxygen (O2) and the two

Table 2 Selected bonding parameters for $[VO_2(acpy\text{-}inh)]$ (**2**) and $[VO_2(acpy\text{-}bhz)]$ (**4**)

Bond lengths/Å	2	4	Bond angles [a]/°	2	4
V–O(1)	1.615(3)	1.615(2)	O1–V–O2	102.95(10)	102.97(10)
V–O(3)		1.618(2)	O1–V–O1#/O3	110.22(19)	110.35(10)
V–O(2)	1.961(3)	1.955(2)	O3–V–O2		102.29(8)
V–N(1)	2.107(3)	2.111(2)	O1–V–N2	124.62(10)	124.03(9)
V–N(2)	2.107(4)	2.104(2)	O3–V–N2		125.17(9)
O(3)–C(8)	1.296(6)	1.300(3)	O2–V–N2	73.59(14)	73.56(7)
N(2)–C(6)	1.294(5)	1.294(3)	O1–V–N1	95.92(11)	96.19(9)
N(2)–N(3)	1.384(5)	1.381(3)	O3–V–N1		96.29(9)
N(3)–C(8)	1.311(6)	1.314(3)	O2–V–N1	146.55(15)	146.51(7)
			N1–V–N2	72.97(15)	72.96(7)
			V–O2–C8	117.4(3)	118.39(15)
			C6–N2–N3	119.9(4)	119.62(19)
			C6–N2–V	121.6(3)	122.19(15)
			N3–N2–V	118.5(3)	118.18(14)
			O2–C8–N3	124.9(5)	123.1(2)
			O2–C8–C9	117.7(4)	118.4(2)

[a] Due to symmetry restrictions, there is no O3 in compound **2**. O3 in **4** corresponds to O1# in **2**.

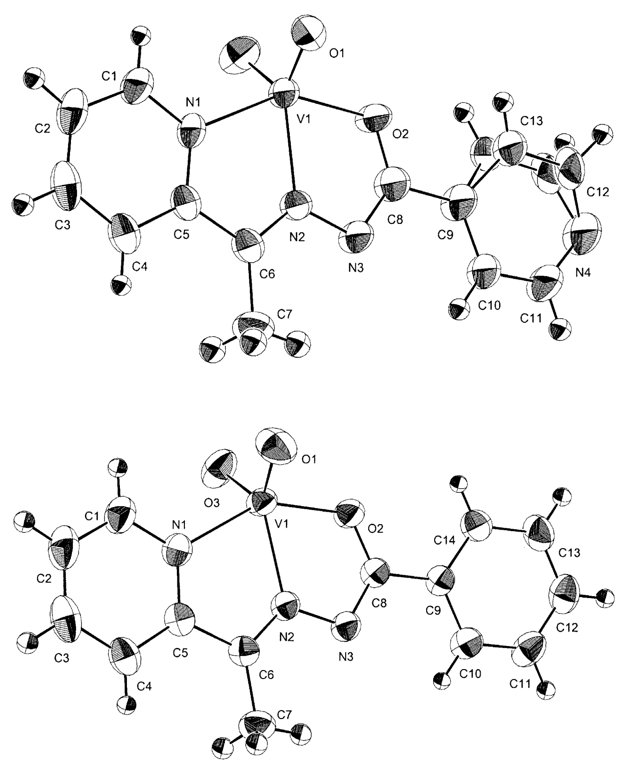

Fig. 2 ORTEP plots (35% probability level) and numbering schemes for **2** and **4**.

N functions (N1, N2) forming the tetragonal plane. There are substantial distortions towards a trigonal bipyramid, quantified by a τ parameter of 0.37 ($\tau = 0$ for an ideal tetragonal pyramid; $\tau = 1$ for an ideal trigonal bipyramid). The distortion thus compares to that in $[VO_2L]$, where HL is a Schiff base derived from 2-hydroxy-1-naphthaldehyde and 8-aminoquinoline,[23] or another type of penta-coordinated hydrazonate.[25] In $[VO_2L]$ complexes with an ideally square-pyramidal geometry, there is a distinct tendency towards dimerisation to $[VOL(\mu\text{-}O)]_2$ with octahedral arrangement.[22,26,27] Examples of trigonal-bipyramidal vanadium complexes are also known.[26,28]

IR spectra. The complexes display a sharp band in the 946–968 cm^{-1} region due to the ν(V=O) mode. In the case of **2** and **4**, there are two such bands between 899 and 946 cm^{-1} due to *cis*-$[VO_2]$ structure, as noted previously by other workers for similar complexes.[29] The peroxo complexes **5** and **6** show three IR active vibrational modes associated with the $[V(O_2)]^{2+}$ moiety at 562–574, 701–714 and 921–926 cm^{-1}, which are assigned to the symmetric $V(O_2)$ stretch (ν_2), the antisymmetric $V(O_2)$ stretch (ν_3) and the O–O intra-stretching (ν_1) mode, respectively.[30] The presence of these bands confirms the η^2-coordination of the peroxo group.

The IR spectra of the ligands exhibit two bands in the regions 3200–3230 and 1653–1661 cm^{-1} due to ν(NH) and ν(C=O) stretches. The absence of these bands in the spectra of all complexes is consistent with the enolisation of the amide functionality and subsequent proton replacement by the metal ion. A new band appearing in the 1235–1274 cm^{-1} range is assigned to the ν(C–O)(enolic) mode. Unequivocal assignment of the ν(C=N) (azomethine) as well as ν(C=C) (ring) stretches of the ligands could not be carried out due to the complexity of the spectra in the 1600 cm^{-1} region. However, the appearance of a sharp band between 1593 and 1608 cm^{-1} should indicate the coordination of both nitrogen atoms. The band due to ν(N–N) mode appears at 991 cm^{-1} in Hacpy-inh, and at 976 cm^{-1} in Hacpy-bhz. This band which, on coordination of the ligands, shifts up to 50 cm^{-1} to higher wave numbers with respect to the free ligand, falls within the range commonly observed for the monodentate coordination of the >N–N< residue.[31] The high frequency shift is expected because of diminished repulsion between the lone pairs of adjacent nitrogen atom.[32] The absence of the band corresponding to the ν(NH) and ν(OH) stretches in the complexes **9** and **10** of benzohydroxamic acid (Hbha) is indicative of the enolisation of the –C=O group of Hbha and subsequent replacement of H by the metal ion. In addition, these complexes exhibit a weak but broad band covering the region 2500–2800 cm^{-1}, which suggests intermolecular hydrogen bonding. Catechol complexes do not show any band due to ν(OH) and thus confirm the coordination of catecholate to the metal ion.

Solution studies

Electronic absorption spectra. Table 3 lists electronic spectral data for the ligands and various complexes. The visible absorption spectra of all complexes are dominated by an intense absorption at 378–392.5 nm and are assigned to a ligand-to-metal charge transfer (LMCT) band. The intra-ligand band at *ca.* 370 nm merges with this band. Benzohydroxamate and catecholate usually induce strong charge transfer to a high valent metal centre. The new band at *ca.* 550 nm in **9** and **10**, and two intense bands at *ca.* 778 and 516 nm in **7** and **8** are thus con-

Table 3 Electronic absorption spectra

Compound (solvent)	λ_{max}/nm (ε/M^{-1} cm^{-1})
Hacpy-inh (DMF)	211.5(21387), 240(11140), 293(14895), 369(3038)
[VO(acpy-inh)acac], **1** (DMF)	275(13783), 385(10661)
(MeOH)	205(11200), 243(7100), 282(7238), 370(4450)
[VO_2(acpy-inh)], **2** (DMF)	269.5(13783), 386.5(5221.6)
[VO(O_2)(acpy-inh)], **5** (DMF)	242(12030), 273.5(12270), 385(7053), 410(sh)(4890)
[VO(acpy-inh)cat], **7** (MeOH)	214.5(39522), 379(17010), 516.5(6460), 778(6608)
[VO(acpy-inh)bha], **9** (MeOH)	214(28414), 378(12025), 551(2958)
Hacpy-bhz (DMF)	205.5(18060),229.5(11835),295.5(21660),367(2007)
[VO(acpy-bhz)acac], **3** (DMF)	275.5(15162), 389(11527)
(MeOH)	379(6515), 292(16110), 205(23320)
[VO_2(acpy-bhz)], **4** (DMF)	392.5(22041), 274(18999), 236(4703), 202.5(6683)
[VO(O_2)(acpy-bhz)] **6** (DMF)	392.5(20310), 268.5(17538), 255.5(6613)
[VO(acpy-bhz)cat] **8** (MeOH)	777(4880), 516(4087), 388.5(22830), 219.5(38040)
[VO(acpy-bhz)bha] **10** (MeOH)	550(4325), 388.5(14551), 249.5(23160), 211.5(32632)

Table 4 ^{1}H NMR spectra (δ in ppm) of ligands and complexes[a]

Compound	NH	CH_3	Aromatic protons
Hacpy-inh	11.19(s, 1H)	2.51(s, 3H)	7.45–8.76(m, 8H)
[VO_2(acpy-inh)], **2**		2.80(s, 3H)	7.78(m, 5H), 8.76–8.83(m, 3H)
[VO(O_2)(acpy-inh)], **5**		2.71(s, 3H)	7.94–8.81(m, 7H), 9.60–9.63(d, 1H)
[VO(acpy-inh)cat], **7**		2.71, 2.82(s each, 3H)	6.58–6.73(m, 4H), 7.79–8.82(m, 8H)
[VO(acpy-inh)bha], **9**		2.74, 2.82(s each, 3H)	7.40–8.76(m, 13H)
Hacpy-bhz	10.90(s, 1H)	2.51(s, 3H)	7.43–8.61(m, 9H)
[VO_2(acpy-bhz)], **4**		2.78(s, 3H)	7.48–8.40(m, 9H)
[VO(O_2)(acpy-bhz)], **6**		2.77(s, 3H)	7.48–8.84(m, 9H)
[VO(acpy-bhz)cat], **8**		2.77, 2.78(s each, 3H)	6.58–6.73(m, 4H), 7.48–8.83(m, 9H)
[VO(acpy-bhz)bha], **10**		2.71, 2.81(s each, 3H)	7.40–8.47(m, 14H)

[a] Letters given in parentheses indicate the signal structure: s = singlet, d = doublet, m = multiplet.

sidered LMCT transitions originating from oxamate oxygens[33] or phenolate oxygen.[34] As vanadium(V) complexes have a 3d° configuration, d–d bands are not expected. However, such d–d transitions appear at *ca.* 600 nm in complexes **1** and **3** as a very weak band.

^{1}H NMR spectra. The coordinating modes of the ligands were also confirmed by recording ^{1}H NMR spectra of the ligands as well as complexes. As presented in Table 4, the sharp signal appearing at 11.19 (in Hacpy-inh) and 10.90 ppm (in Hacpy-bhz) due to the hydrazone NH proton, disappears in the spectra of the complexes, which suggests the conversion of the keto to the tautomeric enol group and subsequent coordination of the enolate oxygen. Aromatic protons of the ligands as well as the complexes appear well within the expected range. The aromatic protons of the coordinated catecholate (in **7** and **8**) give rise to two multiplets in the 6.58–6.73 ppm region, while in the benzohydroxamate complexes **9** and **10**, the phenyl resonances appear along with other aromatic protons, thus making this region very complex. A downfield shift of ~0.2 ppm of the methyl proton signals in comparison to those of the free ligands demonstrates the coordination of the azomethine nitrogen. The methyl region of the catecholate and benzohydroxamate complexes exhibits at least two signals for methyl protons. One of them appears at the same position as observed in the corresponding dioxo complexes, while the other one is new and is due to the authentic mixed ligand complexes. Apparently, slow decomposition of these complexes occurs to give dioxo species.

^{13}C NMR spectra. Assignments of the relevant peaks recorded for the ligands and complexes are presented in Table 5. A large coordination-induced shift $\Delta\delta$ = [δ(complex) – δ(free ligand)] of the signals for the carbon atoms in the vicinity of the coordinating atoms (*e.g.* the azomethine carbon C1 and the enolate carbon C7) demonstrate their coordination.[35] Even the methyl carbons associated with the azomethine group give rise to some downfield shift. The coordination of catecholate is reflected by the appearance of a new peak at 145.3 in **7** and at 148.6 in **8**, while coordination of benzohydroxamate is confirmed by the appearance of at least two new peaks in the 165–180 ppm region. Several additional peaks of low intensity in the 120–130 ppm region for the complexes **7** to **10** correspond to the respective dioxo complexes formed by partial decomposition (see also above and below).

^{51}V NMR spectra. Table S1 (ESI) presents ^{51}V NMR spectral data of the complexes. The resonances have line widths at half-height of approximately 200 Hz, which is still considered as narrow in ^{51}V NMR spectroscopy. The dioxovanadium(V) complexes **2** and **4** exhibit one strong resonance at *ca.* −507, an expected value for the dioxovanadium(V) complexes having a mixed *O*/*N* donor set.[36] The catecholato complexes **7** and **8** display two bands: one in the 319–362 ppm region characteristic of catecholate coordination,[34] and a second peak in the range of dioxo species, again showing that partial decomposition occurs in solution. Similarily, complexes **9** and **10** display two bands in the 51 to 71 and at −506 to −507 ppm region. The former resonance belongs to the complexes **9** and **10** while the latter is due to decomposition to **2** and **4**. In some of the solutions, there is an additional minor resonance around −590, which coincides with the chemical shift of the authentic oxo–peroxo complexes **5** and **6**. These resonances do not appear under strict exclusion of air, suggesting that some redox chemistry takes place between the vanadium complexes and oxygen in solution.

EPR studies. DMSO solutions of the complexes [VOL(acac)] (**1** and **3**) provide EPR patterns with a g_0 value of 1.957 and the following hyperfine coupling constants: **1**: $A_0 = 98.7$, $A_z = 175.3$, $A_{xy} = 60.2 \times 10^{-4}$ cm^{-1}; **3**: $A_0 = 99.7$, $A_z = 180.3$, $A_{xy} = 58.9 \times 10^{-4}$ cm^{-1}. Practically the same values have been obtained in MeCN. If compared with EPR parameters of other VO^{2+} complexes

Table 5 ^{13}C NMR chemical shift (δ in ppm); see scheme below for atom numbering

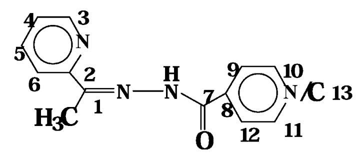

Compound	CH_3	C1	C7	C2	C6	C9/C12	C10/C11	C3/C4/C5/C8/C13
Hacpy-inh	12.94	154.92	162.83	156.29	148.71	136.72	150.14	119.81, 120.58, 122.0, 122.97, 124.49, 141.3
$[VO(O_2)(acpy\text{-}inh)]$, **5**	13.29	155.62	174.54	156.34	149.40	142.06	150.37	122.35, 124.96, 126.97, 139.9
$(\Delta\delta)^a$	(0.35)	(0.70)	(11.71)					
$[VO(acpy\text{-}inh)cat]^b$, **7**	13.74	162.20	173.5	153.99	148.68	142.34	150.48	115.65, 119.24, 122.27, 126.08, 128.61, 145.26
$(\Delta\delta)$	(0.80)	(6.58)	(10.67)					
$[VO(acpy\text{-}inh)bha]^b$, **9**	13.42	163.70	173.5	157.2	154.0	142.27	150.53	122.32, 125.19, 126.40, 127.84, 128.85, 129.76, 131.35, 135.22, 139.56
$(\Delta\delta)$	(0.48)	(8.78)	(10.67)					
Hacpy-bhz	12.60	155.14	164.21	147.82	148.65	136.64	128.30	120.39, 124.17, 131.63, 133.98
$[VO_2(acpy\text{-}bhz)]$, **4**	13.63	163.37	175.99	152.98	154.68	143.15	128.66	125.71, 127.03, 130.82, 132.36
$(\Delta\delta)$	(1.03)	(8.14)	(11.78)					
$[VO(O_2)(acpy\text{-}bhz)]$, **6**	13.68	163.43	176.03	153.03	154.73	143.30	128.71	125.76, 127.08, 130.86, 132.41
$(\Delta\delta)$	(1.08)	(8.29)	(11.82)					
$[VO(acpy\text{-}bhz)cat]^b$, **8**	13.52	159.95	175.53	153.0	154.29	142.21	128.91	125.85, 126.26, 127.04, 128.16, 131.01, 131.4, 132.27, 132.38, 148.56
$(\Delta\delta)$	(0.92)	(4.81)	(11.32)					
$[VO(acpy\text{-}bhz)bh)]^b$, **10**	13.25	161.21	175.54	154.20	156.08	142.70	128.89	124.70, 125.88, 126.56, 127.77, 128.15, 129.79, 131.20, 132.50, 135.30
$(\Delta\delta)$	(0.65)	(6.07)	(11.33)					

^{a} $\Delta\delta = \delta$(complex) − δ(free ligand). ^{b} Another set of signals for all carbons also appears and their positions are nearly identical to those of the dioxo species.

having a mixed *ON* donor set,[37] the low g and high A_z values are noticeable, and possibly account for diminished delocalisation of spin density into the ligand system as a consequence of the substantial distortion in the molecules.

Stability studies. The stability of complexes **7**, **8**, **9** and **10** in various solvents were studied. Solutions of these complexes are stable for about a week in dry CH_2Cl_2 and for about two days in methanol, but – as already evidenced by the spectral studies – they slowly decompose in DMF and DMSO. The conversion of the $[VO]^{2+}$ complexes **7** and **8** into the $[VO_2]^+$ species with the loss of the bidentate ligand catecholate(2−) was established by electronic absorption studies of DMSO solutions, Fig. 3. In dry DMSO conversion is rather slow and takes about 24 h. During this period, a gradual loss in intensity of the LMCT bands due to coordinated catecholate and their final disappearance is observed. Addition of water facilitates this conversion. In a typical experiment, addition of 1 drop of H_2O in 5 ml of ~10^{-4} M solution of **7** gives rise to complete conversion into **2** within 8 h, as illustrated in Fig. 3. Similar observations have also been noted in oxovanadium(V) complexes containing catecholates along with Schiff bases derived from salicylaldehyde and 8-aminoquinoline.[23] Eqn. (8) represents the decomposition reaction.

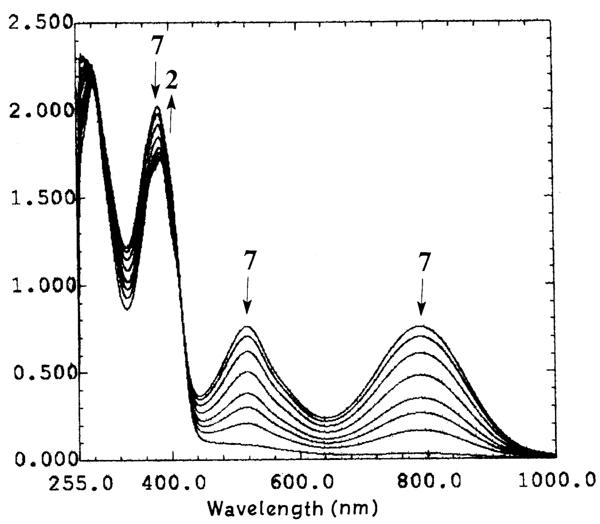

Fig. 3 Absorption spectra of [VO(acpy-inh)cat] (**7**) in DMSO (*ca.* 10^{-4} M solution) plus one drop of H_2O as a function of time over a period of 8 h.

$$[VO(acpy\text{-}inh)cat] + H_2O \longrightarrow [VO_2(acpy\text{-}inh)] + H_2cat \quad (8)$$

Reaction of 7 with L-ascorbic acid. The reactivity of complex **7** towards L-ascorbic acid was monitored by electronic absorption spectroscopy. In a typical reaction, **7** (10^{-4} M solution in CH_2Cl_2) was treated with L-ascorbic acid dissolved in the minimum amount of MeCN in an approximately 1 : 2 molar ratio. The two LMCT bands at 790 and 518 nm slowly disappeared. The 379 nm band experiences a slight red shift, while the 274 nm band sharpens. The spectra recorded at different intervals of time are shown in Fig. 4. Since catecholato and benzohydroxamato complexes are stable in CH_2Cl_2 and CH_2Cl_2–MeCN for several days, any change in the absorption spectra should come about by the reaction between L-ascorbic acid and the complex. As L-ascorbic acid has reducing properties, intermediate reduction of **7** with concomitant removal of coordinated catecholate may occur. The matching of the final spectrum with the dioxovandium(V) complex **2** indicates that V^{IV} is reoxidised to form $[VO_2L]$. The net reaction is thus an oxidation of ascorbic acid by atmospheric oxygen, catalysed by V^V.

Reaction of 2 and 4 with HCl. Dioxovanadium(V) complexes can react with acids to give oxo–hydroxo complexes, and the corresponding reaction has also been accomplished for **2** and **4** with HCl. Addition of methanol saturated with HCl gas to **2** dissolved in DMF causes darkening of the solution, accompanied by a slight reduction in intensity of the 274 nm band, as illustrated in Fig. 5. Further addition of HCl results in an

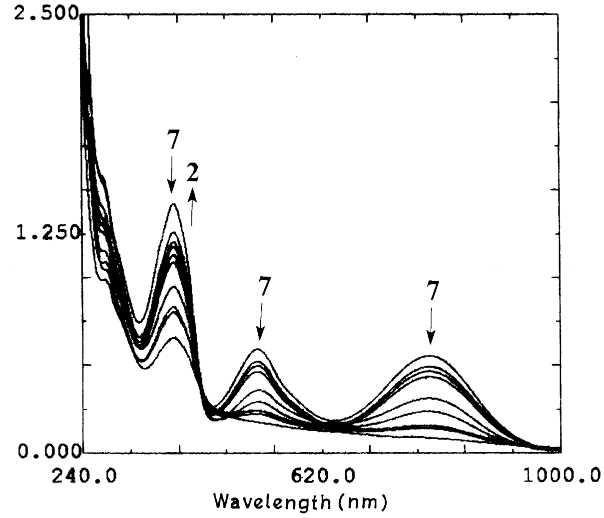

Fig. 4 Absorption spectra of *ca.* 10^{-4} M CH_2Cl_2 solution of [VO(acpy-inh)cat] (**7**) in the presence of L-ascorbic acid (dissolved in a minimum amount of MeCN) in a 1 : 2 molar ratio as a function of time over a period of 2 h.

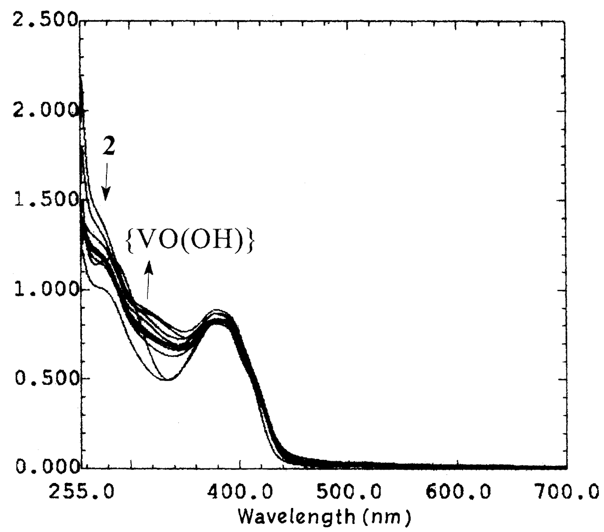

Fig. 5 Titration of [VO_2(acpy-inh)] (**2**) with a saturated solution of HCl in methanol; the spectra were recorded after the addition of five drops portions of methanol–HCl to 10 ml of a *ca.* 10^{-4} M DMF solution of **2**.

increase in intensity of the 274 nm band along with its broadening. In addition, a shoulder starts to appear at *ca* 324 nm. The 384 nm band remains nearly constant. Following the formation of an oxo–hydroxo complex, *viz.* $[VO(OH)HL]^+$, where H_2L = *N*-[{(*o*-hydroxyphenyl)methyl}-*N′*-(2-hydroxyethyl)ethylenediamine], generated with HCl from the respective dixoxvanadium(V) dimer,[38] and based on established hydroxo–oxovanadium complexes,[39,40] the formation of $[VO(OH)(acpy\text{-}inh)]^+$ is also proposed here. On allowing the solution to stand overnight, or on addition of KOH dissolved in methanol, the reaction is reversed, *i.e.* the solution acquires the original spectral pattern of **2**. The formation of a hydroxo species is an important observation in the context of the vanadate-dependent haloperoxidases, for which a hydroxo group in an apical position has been confirmed.[41]

Conclusion

Monomeric, distorted square-pyramidal dioxovanadium(V) complexes have been obtained by using bulky monobasic tridentate *ONN* ligands based on hydrazones. These can be looked at as structural models for the active site in vanadate-dependent haloperoxidases. Intermediate species containing the $[VO(OH)^{2+}]$ core can be obtained by protonation of dioxo complexes. One of the oxo-groups can also be replaced by peroxide to form oxoperoxo complexes, another feature which is pertinent to the peroxidases. Electron transfer processes are modeled with the complex [VO(acpy-inh)cat] in the presence of ascorbic acid and air, yielding $[V^VO_2L]$ possibly *via* a $[V^{IV}OL]^+$ intermediate.

Acknowledgements

M. R. M. and S. K. are thankful to the Council of Scientific and Industrial Research, New Delhi 110 012, India for financial support of the work. We also wish to thank the RSIC, Central Drug Research Institute, Lucknow, India, for providing elemental analyses of the complexes. This work was further supported by the Deutsche Forschungsgemeinschaft and the Fonds der Chemischen Industrie.

References

1 *Vanadium and its Role in Live, Metal Ions in Biological Systems*, eds. H. Sigel and A. Sigel, Marcel Dekker, New York, 1995, vol. 31; *J. Inorg. Biochem.*, 2000, **80** (special issue dedicated to biological aspects of vanadium).

2 D. Rehder, *Coord. Chem. Rev.*, 1999, **182**, 297.

3 A. Butler, *Coord. Chem. Rev.*, 1999, **187**, 17.

4 H. B. ten Brink, A. Tuyman, H. L. Dekker, W. Hemrika, Y. Izumi, T. Oshiro, H. E. Shoemaker and R. Wever, *Inorg. Chem.*, 1998, **37**, 6780; M. A. Andersson and S. G. Allenmark, *Tetrahedron*, 1998, **54**, 15293.

5 A. Butler and C. J. Carrano, *Coord. Chem. Rev.*, 1991, **109**, 61.

6 B. J. Hamstra, G. J. Colpas and V. L. Pecorao, *Inorg. Chem.*, 1998, **37**, 949; Y. Zhang and R. H. Holm, *Inorg. Chem.*, 1990, **29**, 911; A. Butler and A. H. Baldwin, *Struct. Bonding (Berlin)*, 1997, **89**, 109.

7 V. Conte, F. Di Furia and G. Licini, *Appl. Catal.*, 1997, **157**, 335.

8 C. Hiort, J. Goodisman and J. C. Dabrowiak, *Biochemistry.*, 1996, **35**, 12354.

9 M. J. Clague, N. L. Keder and A. Butler, *Inorg. Chem.*, 1993, **32**, 4754; G. J. Colpas, B. J. Hamstra, J. W. Kampf and V. L. Pecoraro, *J. Am. Chem. Soc.*, 1996, **118**, 3478; M. Bhattarcharjee, S. Ganguly and J. Mukherjee, *J. Chem. Res. (S)*, 1995, 80; R. M. Tótaro, P. A. M. Williams, M. C. Apella, M. A. Blesa and E. J. Baran, *J. Chem. Soc., Dalton Trans.*, 2000, 4403.

10 I. W. C. E. Arends, M. P. Birelli and R. A. Sheldon, *Stud. Surf. Catal.*, 1997, **110**, 1031.

11 C. Bolm and F. Bienewald, *Angew. Chem., Int. Ed. Engl.*, 1995, **34**, 2640; A. H. Vetter and A. Berkessel, *Tetrahedron Lett.*, 1998, **39**, 1741; D. A. Cogan, G. Liu, K. Kim and B. J. Ellmon, *J. Am. Chem. Soc.*, 1998, **120**, 8011; W. Adam, D. Golsch, J. Sundermeyer and G. Wahl, *Chem. Ber.*, 1996, **129**, 1177; K. Nakajima, K. Kojima, M. Kojima and J. Fujita, *Bull. Chem. Soc. Jpn.*, 1990, **63**, 2620; D. Rehder, G. Santoni, G. M. Licini, C. Schulzke and B. Meier, *Coord. Chem. Rev.*, in the press.

12 K. H. Thompson, J. H. McNeil and C. Orvig, *Chem. Rev.*, 1999, **99**, 2561; M. Melchior, K. H. Thompson, J. M. Jong, S. J. Retting, E. Shuter, V. G. Yuen, Y. Zhou, J. H. McNeil and C. Orvig, *Inorg. Chem.*, 1999, **38**, 2288; S. S. Amin, K. Cryer, B. Zhang, S. K. Dutta, S. S. Eaton, O. P. Anderson, S. S. Miller, B. A. Reul, S. M. Brichard and D. C. Crans, *Inorg. Chem.*, 2000, **39**, 406.

13 D. Rehder, J. Costa Pessoa, C. F. G. C. Geraldes, M. M. C. A. Castro, T. Kabanos, T. Kiss, B. Meier, G. Micera, L. Pettersson, M. Rangel, A. Salifoglou, I. Turel and D. Wang, *J. Biol. Inorg. Chem.*, 2002, **7**, 384.

14 C. R. Cornman, G. J. Colpas, J. D. Hoeschele, J. Kampf and V. L. Pecoraro, *J. Am. Chem. Soc.*, 1992, **114**, 9925.

15 S.-X. Liu and S. Gao, *Inorg. Chim. Acta*, 1998, **282**, 149 and literature cited therein.

16 S. W. Taylor, B. Kammerer and E. Bayer, *Chem. Rev.*, 1997, **97**, 333.

17 I. Batinić-Haberle, M. Biruš and M. Pribanič, *Inorg. Chem.*, 1991, **30**, 4882.

18 R. A. Row and M. M. Jones, *Inorg. Synth.*, 1957, **5**, 113.

19 G. M. Sheldrick, SHELXS 86, University of Göttingen, 1986; G. M. Sheldrick, SHELXS 93, University of Göttingen, 1993.

20 O. W. Howarth, *Progr. Nucl. Magn. Reson Spectrosc.*, 1991, **22**, 453.
21 H. Schmidt, I. Andersson, D. Rehder and L. Pettersson, *Chem. Eur. J.*, 2001, **7**, 251.
22 C. J. Carrano, C. M. Nunn, R. Quan, J. A. Bonadies and V. L. Pecoraro, *Inorg. Chem.*, 1992, **29**, 944.
23 G. Asgedom, A. Sreedhara, J. Kivikoski, E. Kolehmainen and C. P. Rao, *J. Chem. Soc., Dalton Trans.*, 1996, 93.
24 S. N. Pal and S. Pal, *Acta Crystallogr., Sect. C*, 2001, **57**, 141.
25 M. R. Maurya, S. Khurana, W. Zhang and D. Rehder, *Eur. J. Inorg. Chem.*, 2002, 1749; M. R. Maurya, S. Khurana, C. Schulzke and D. Rehder, *Eur. J. Inorg. Chem.*, 2001, 779; D. Wang, M. Ebel, C. Schulzke, C. Grüning, S. K. S. Hazari and D. Rehder, *Eur. J. Inorg. Chem.*, 2001, 935.
26 G. Asgedom, A. Sreedhara, J. Kivikoski and C. P. Rao, *Polyhedron*, 1997, **16**, 643.
27 H. Schmidt, M. Bashirpoor and D. Rehder, *J. Chem. Soc., Dalton Trans.*, 1996, 3865.
28 L. M. Mokry and C. J. Carrano, *Inorg. Chem.*, 1993, **32**, 6119.
29 S. N. Pal and S. Pal, *J. Chem. Crystallogr.*, 2000, **30**, 329; X. Li, M. S. Lah and V. L. Pecoraro, *Inorg. Chem.*, 1988, **27**, 4657; A. G. J. Ligtenbarg, A. L. Spek, R. Hage and B. E. Feringa, *J. Chem. Soc., Dalton Trans.*, 1999, 659.
30 A. D. Westland, F. Haque and J.-M. Bouchard, *Inorg. Chem.*, 1980, **19**, 2255.
31 M. R. Maurya, S. Gopinathan, C. Gopinathan and R. C. Maurya, *Polyhedron*, 1993, **12**, 159.
32 S. P. Perlepes, D. Nicholls and M. R. Harrison, *Inorg. Chim. Acta*, 1985, **102**, 137.
33 S. Gao, Z.-Q. Weng and S.-X. Liu, *Polyhedron*, 1998, **15**, 3595.
34 G. Asgedom, A. Sreedhara and C. P. Rao, *Polyhedron*, 1996, **15**, 3731; C. R. Cornman, J. Kampf and V. L. Pecoraro, *Inorg. Chem.*, 1992, **31**, 1981.
35 A. D. Keramidas, A. B. Papaioannou, A. Vlahas, T. A. Kabanos, G. Bonas, A. Makriyannis, C. P. Rapropoulou and A. Terzis, *Inorg. Chem.*, 1996, **35**, 357.
36 D. Rehder, C. Weidemann, A. Duch and W. Priebsch, *Inorg. Chem.*, 1988, **27**, 584; D. Rehder, in *Transtion Metal Nuclear Magnetic Resonance*, ed. P. S. Pregosin, Elsevier, New York, 1991 p. 1.
37 A. J. Tasiopoulos, A. N. Troganis, A. Evangelou, C. P. Raptopoulos, A. Terzis, Y. Deligiannakis and T. A. Kabanos, *Chem. Eur. J.*, 1999, **5**, 910; C. R. Cornman, J. Kampf, M. S. Lah and V. L. Pecoraro, *Inorg. Chem.*, 1992, **31**, 2035.
38 G. J. Colpas, B. J. Hamstra, J. W. Kampf and V. L. Pacoraro, *Inorg. Chem.*, 1994, **33**, 4669.
39 M. Kosugi, S. Hikitchi, M. Akita and Y. Moro-oka, *Inorg. Chem.*, 1999, **38**, 1173.
40 P. Knopp, K. Wieghardt, B. Nuber, J. Weiss and W. S. Sheldrick, *Inorg. Chem.*, 1990, **29**, 363; A. Giacomelli, C. Floriani, A. O. de Souza Duarte, A. Chiesi-Villa and C. Guastino, *Inorg. Chem.*, 1982, **21**, 3310.
41 M. Weyand, H.-J. Hecht, M. Keiß, M.-F. Liaud, H. Vilter and D. Schomburg, *J. Mol. Biol.*, 1999, **293**, 595.